TEMPERATURE SIMULATION OF A REACH OF THE METHOW RIVER NEAR WINTHROP, WASHINGTON

Jianchun Huang, Ph.D., P.E., Hydraulic Engineer, Bureau of Reclamation, Denver, CO, vhuang@usbr.gov; Jennifer Bountry, M.S., P.E., Hydraulic Engineer, Bureau of Reclamation, Denver, CO, jbountry@usbr.gov

Abstract: In this paper, a two-dimensional (2D) temperature model is tested within a reach of the Methow River near Winthrop, WA. The reach has a warm water tributary entering on river left and a cold water spring entering from river right. The 2D temperature model is spatially distributed in the lateral and longitudinal geographic extents, allowing for more accurate simulation of lateral changes in temperature across the channel than a 1D representation. The SRH-2D temperature model utilizes meteorological data as inputs (solar radiation, cloud cover, air temperature, dew point temperature, air pressure, and wind speed). Physical processes modeled include solar and atmospheric heating, effects of terrain and vegetation shading, heat exchange between water column and bed substrate, and losses due to evaporation, conduction, and back radiation. Two sets of data are used to test the model. Test one uses steady solution to simulate the lateral temperature mixing zone when warmer water from the Chewuch River enters from river left and colder water from Spring Creek enters from river right. Test two uses unsteady solution to simulate the continuous temperature change due to various water heat gains and losses.

INTRODUCTION

Lai and Mooney (2009) developed a two-dimensional (2D) temperature module for an existing 2D hydraulic and sediment transport model, SRH-2D. The 2D model incorporates data with both lateral and longitudinal geographic extents rather than lumping results into a point-to-point or uni-directional representation. The improved representation of spatial features allows more accurate simulation of lateral changes in temperature across the channel. The SRH-2D temperature model utilizes meteorological data as inputs (solar radiation, cloud cover, air temperature, dew point temperature, air pressure, and wind speed). Physical processes modeled include solar and atmospheric heating, effects of terrain and vegetation shading, heat exchange between water column and bed substrate, and losses due to evaporation, conduction, and back radiation.

In this research, the SRH-2D temperature model was verified in a reach of the Methow River near Winthrop, WA. The Methow River reach has a warmer water tributary entering on river left and a colder water spring entering from river right. Two sets of data were used to test the model. Test one involved using thermal infrared remote-sensing (TIR) imagery data that represents a grid of surface temperatures at a single river flow and a single point in time. This data was used to test how well the model can represent lateral changes in temperature across the channel. Surface water temperature can be different than depth-averaged temperature, which is computed by the 2D model. This difference may cause some variance in how well the 2D model results represent the TIR data, particularly in areas where the mixing rate of the river is slow or highly variable (due to stratification effects). However, the Methow is generally well mixed due to a steep slope and fairly shallow depths. Test two used three temperature loggers that provide continuous data over several months from spring to fall. The loggers provided a test of how well the model could represent temporal and longitudinal changes in temperature.

TEMPERATURE MODEL

Temperature Equation: The 2D depth-averaged flow equations are based on the assumptions that stream flows are shallow compared to width and the effect of vertical motion is negligible.
Conservation of thermal energy leads to the 2D depth-averaged temperature equation expressed as:

$$\frac{\partial hT}{\partial t}+\frac{\partial hUT}{\partial x}+\frac{\partial hVT}{\partial y}=\frac{\partial}{\partial x}\left[\frac{h\nu_t}{\sigma_t}\frac{\partial T}{\partial x}\right]+\frac{\partial}{\partial y}\left[\frac{h\nu_t}{\sigma_t}\frac{\partial T}{\partial y}\right]+\frac{\Phi_{net}}{c_w\rho_w}+\frac{q_{sp}}{A_{sp}}\left(T_{sp}-T\right) \quad (1)$$

In the above, T is depth averaged water temperature [C], x and y are horizontal Cartesian coordinates [m], t is time [s], h is water depth [m], U and V are depth-averaged velocity components [m/s] in x and y directions, respectively, ν_t is the turbulent viscosity and dispersion [m^2/s], σ_t is the turbulent Prandtl number, ρ_w is the water density [kg/m^3], $c_w$is the specific heat of water [J/kg/C], q_{sp} is the spring water flow rate [m^3/s] into the stream (zero if

spring flows out), A_{sp} is the area [m^2] of the spring water inflow, T_{sp} is the spring water temperature [C], and Φ_{net} is the net heat exchange [w/m^2] between water column and its surroundings (through water surface and streambed). The turbulent eddy viscosity (ν_t) is computed with a turbulence model (Rodi, 1993). The net heat flux, Φ_{net}, consists of six contributions as follows:

$$\Phi_{net} = \Phi_{ns} + \Phi_{na} + \Phi_{bed} - \Phi_{br} - \Phi_e - \Phi_c \tag{2}$$

where

Φ_{ns}= net solar radiation entering water surface;
Φ_{na}= net atmospheric radiation entering water surface;
Φ_{br}= heat loss by back radiation from stream (black body radiation);
Φ_e= evaporative heat loss at water surface;
Φ_c= conductive heat loss at water surface; and
Φ_{bed} = heat flux into stream at channel bed.

Solar Radiation: If measured solar radiation (Φ_{sm}) at water surface is available, the net solar radiation is computed as (Hauser and Schohl, 2003)

$$\Phi_{ns} = \Phi_{sm} R_s \tag{3}$$

where Φ_{sm} is measured solar radiation (shade free solar radiation at the water) and R_s is reflection and terrain and vegetation shading factor which is computed by the following equations (Hauser and Schohl, 2003):

$$R_s = \begin{cases} R_{sm} & \text{if } X_n \le B \text{ (shade free)} \\ 0.2 & \text{if } X_n > B+W \text{ (full shade)} \\ R_{sm}\frac{B+W-X_n}{W} + 0.2\frac{X_n-B}{W} & \text{if } B < X_n \le B+W \text{ (partial shade)} \end{cases} \tag{4}$$

In the above:

$R_{sm} = 1 - a(57.3\alpha)^{-b}$ = shade-free reflection factor (a and b see Table 1);
α = solar altitude in radians;
W = width of the stream cross section;
B = distance from trees to water edge;
$X_n = H_b \cos\beta / \tan\alpha$ = normal distance from trees to shadow edge;
H_b = tree and bank height from water surface;
$\beta = |\theta - 90/57.3|$ = angle between sun and stream axis normal in radian;
$\theta = \left|A_{zs} - \frac{A_{zr}}{57.3}\right|$ = angle between sun and stream axis in radian;
A_{zr}= river azimuth, clockwise from north to direction of flow in degree;
A_{zs} = sun azimuth in radian calculated by $\cos A_{zs} = -\frac{\sin\phi\sin\alpha - \sin\delta}{\cos\phi\cos\alpha}$.
ϕ = site latitude in radians; and
δ = is sun declination (between the sun and equator) in radians.

Table 1 Coefficients of solar radiation reflection.

Cloud Cover C	a	b
0-0.05	1.18	0.77
0.05 – 0.5	2.20	0.97
0.5 – 0.92	0.95	0.75
0.92 – 1.0	0.35	0.45

The solar altitude α is computed assuming spherical geometry, as follows (Huber and Harleman, 1968):

$$\sin\alpha = \sin\phi\sin\delta + \cos\phi\cos\delta\cos h \tag{5}$$

where ϕ is site latitude in radians, δ is sun declination in radians, and h is the sun hour angle in radians. If no measured solar radiation (Φ_{sm}) is available, the solar radiation that reaches the water surface can be estimated from (Martin and McCutcheon, 1999)

$$\Phi_{sm} = H_0 a_t C_a \tag{6}$$

where H_0 = the amount of radiation reaching the earth's outer atmosphere (Wm^{-2}); a_t= radiation scattering and absorption factor; C_a = the fraction of solar radiation not absorbed by clouds.
The fraction of solar radiation passing through the clouds is given by the cloud cover (C) as

$$C_a = 1 - 0.65C^2 \tag{7}$$

The flux of solar radiation that strikes the earth's outer atmosphere is estimated from

$$H_0 = \frac{H_{sc}}{r^2}[\sin\phi\sin\delta + \frac{12}{\pi}\cos\phi\cos\delta(\sin h_e - sinh_b)]\Gamma \tag{8}$$

H_{sc} = the solar constant (1390 Wm^{-2}); r = the relative distance (-) between the earth and sun; ϕ = the site latitude in radians; δ = sun declination (between the sun and equator) in radians; h_e and h_b = the solar hour angles at the end and the beginning of the time period over which H_0 is being calculated, respectively; and Γ = a correction factor for diurnal exposure to the radiation flux. The relative earth-sun distance can be estimated from

$$r = 1.0 + 0.017\cos\left[\frac{2\pi}{365}(186 - D_y\right] \tag{9}$$

where D_y = the Julian day of the year. The declination of the sun can be estimated from

$$\delta = \frac{23.45\pi}{180}\cos\left[\frac{2\pi}{365}(172 - D_y\right] \tag{10}$$

The hour angles (radians) at the beginning and ending of the period over which H_o is being calculated is computed from

$$h_b = \left\{\frac{\pi}{12}[(h_r - 1) - \Delta t_s + 12a_2]\right\} + b_2(2\pi) \tag{11}$$

$$h_e = \left\{\frac{\pi}{12}[h_r - \Delta t_s + 12a_2]\right\} + b_2(2\pi) \tag{12}$$

where h_r is the hour of the day from 1 to 24; the coefficient a_2 =1.0 for $h_r \leq 12$ and a_2 =-1.0 for $h_r > 12$. The coefficient b_2 varies with the magnitude of the quantity inside the curly brackets for both h_b and h_e in Eqs. (11) and (12). The coefficient b_2 = -1 for $\{\cdot\} > 2\pi$, b_2 = 1 for $\{\cdot\} < 0$, and b_2=0 otherwise.

The fraction of an hour between the standard meridian and the local meridian is Δt_s. In the United States, the standard meridians are at 75°, 90°, 105°, and 120° for eastern, central, mountain, and Pacific Time zones; respectively. The fraction can be calculated from

$$\Delta t_s = \frac{E_a}{15}(L_{sm} - L_{lm}) \tag{13}$$

where L_{sm} is the standard meridian, L_{lm} is the local meridian. $E_a = -1$ for west longitude and $E_a = 1$ for east longitude. For example, at Methow River at Winthrop, $L_{sm} = 120^o$ (Pacific Time zone), $L_{lm} = 120.167639^o$ (longitude of Winthrop), and $E_a = -1$ for west longitude.
The correction factor Γ in Eq.(8) is set to one at day time (between sunrise and sunset) and zero at night time. The standard time of sunset and sunrise can be estimated from

$$t_{ss} = \frac{12}{\pi}\cos^{-1}\left(-\frac{\sin\phi\sin\delta}{\cos\phi\cos\delta}\right) + \Delta t_s + 12 \tag{14}$$

$$t_{su} = -t_{ss} + 2\Delta t_s + 24 \tag{15}$$

The radiation scattering and absorption factor a_t in Eq.(6) can be estimated from

$$a_t = \frac{t + 0.5(1 - s - c_d)}{1 - 0.5R_g(1 - s - c_d)} \tag{16}$$

where c_d is a dust coefficient, which has a range of 0.0 to 0.13 and a typical value of 0.06; and R_g is the reflectivity of the water surface, which varies with the type of cloud cover as

$$R_g = a_3\left(\frac{180}{\pi}\alpha\right)^{b_3} \tag{17}$$

where α is the solar altitude in radians, calculated in Eq.(5) and a_3 and b_3 are coefficients (Table 2) depending on the cloud cover (C).

Table 2 Coefficients a_3 and b_3 describing the reflection of solar radiation at the water surface (source: Martin and McCutcheon, 1999; and Marciano and Harbeck, 1954).

Description	Fraction Cloud Cover (C)	a_3	b_3
Overcast	C> 0.9	0.33	-0.45
Broken	0.5 < C <0.9	0.95	-0.75
Scattered	0.1 <C <0.5	0.5	-0.97
Clear	C < 0.1	1.18	-0.77

The mean atmospheric transmission coefficient s and t in Eq. (16) is given by

$$s = \exp[-(0.465 + 0.134P_{wc})(0.129 + 0.171\exp(-0.88\theta_{am}))\theta_{am}] \tag{18}$$
$$t = \exp[-(0.465 + 0.134P_{wc})(0.179 + 0.421\exp(-0.721\theta_{am}))\theta_{am}] \tag{19}$$

where θ_{am} is the dimensionless optical mass, $P_{wc}$is the mean daily precipitable atmospheric water content, given by

$$P_{wc} = 0.85\exp(0.11 + 0.0614T_d) \tag{20}$$
$$\theta_{am} = \left(\frac{288 - 0.0065Z}{288}\right)^{5.256} / \left[\sin\alpha + 0.15\left(\frac{180\alpha}{\pi} + 3.855\right)^{-1.253}\right] \tag{21}$$

where T_d = the dew point temperature [C], Z = the site elevation (m) and α = the solar altitude in radians, calculated in Eq.(5).

Atmosphere Radiation: The net long-wave radiation (atmospheric radiation entering water surface) is computed as:

$$\Phi_{na} = 5.16432 \cdot 10^{-13}(1 + 0.17C^2)(T_a + 273.16)^6 \tag{22}$$

where C is cloud cover, fraction of the sky covered by clouds, and T_a is dry bulb air temperature [C].

Outgoing Black-Body Radiation: The outgoing black-body radiation emitted from the water surface is a function only of the water temperature, and it is given by (Huber and Harleman, 1968):

$$\Phi_{br} = \varepsilon_w\sigma(T_w + 273.16)^4 \tag{23}$$

where T_w is water-surface temperature [C], ε_w is emissivity (0.97 by Huber and Harleman (1968) and 0.98 by Tung et al. (2006), and σ is Stefan-Boltzman constant (5.672×10^{-8} w/m^2/K^4). In the current model, the depth averaged temperature T is used for T_w.

Evaporative Heat Loss: The evaporative heat loss is computed by:

$$\Phi_e = \rho_w L(a_1 + b_1 W_a)(e_s - e_a) \tag{24}$$

where:

$L = 4184(597 - 0.57T_w)$ =the latent heat [J/kg];
T_w = water surface temperature in Celsius;
W_a = wind speed (m/s);
a_1, b_1 = constants: a_1=0.0 to 4.0e-9; b_1=1.0e-9 to 3.0e-9;
$e_a = 2.171 \times 10^8 \exp\left[-\frac{4157}{T_d + 239.09}\right]$ = saturation vapor pressure [mb];
T_d = dew point temperature in Celsius; and
$e_s = \alpha_j + \beta_j T_w$ = saturation vapor pressure [mb] with coefficients in Table 3

Table 3 Coefficients to compute saturation vapor pressure.

T	j	αj	βj
0-5	1	6.05	0.522
5-10	2	5.10	0.710
10-15	3	2.65	0.954
15-20	4	-2.04	1.265
20-25	5	-9.94	1.659
25-30	6	-22.29	2.151
30-35	7	-40.63	2.761
35-40	8	-66.90	3.511

Conduction Heat Loss to Air: The conduction heat loss is:

$$\Phi_c = 0.61 \times 10^{-3} \rho_w L(a_1 + b_1 W_a) P(T_w - T_a) \tag{25}$$

where P is air barometric pressure [mb] and a_1 and b_1 are defined the same as in Eq.(24), T_w is water surface temperature [C], and T_a is dry bulb air temperature [C].

Heat Exchange with Stream Bed: Heat exchange between stream bed and stream water is significant for shallow streams and it consists of two contributions: conduction from bed to stream and net solar radiation entering bed. It is computed by the following expression:

$$\Phi_{bed} = \frac{k_b}{0.5\delta_b}(T_b - T_w) - (1 - A_b)(1 - \beta)\exp[-\eta(D - 0.6)]\,\Phi_{ns} \tag{26}$$

where k_b is the thermal conductivity of the streambed bed material, $\delta_b$is the effective bed thickness used for heat conduction computation, T_w is the water temperature, T_b is the effective stream bed temperature which is updated each time step by $T_b = T_b^{old} - \frac{\Phi_{\text{bed}}\Delta t}{\rho_b C_b \delta_b}$ with ρ_b and C_b the density and specific heat of the bed materials and Δt is the time step for simulation, A_b is albedo of bed material, β is fraction of solar radiation absorbed in the top 0.6m of surface water, η is extinction coefficient in water [1/m], and D is water depth [m].

RESULTS

Test Case with FLIR Data: Watershed Sciences (2009) provided TIR imagery for approximately 160 river miles in the Methow River Basin for the Yakama Tribe Fisheries. TIR images were collected with a temperature sensor mounted on the underside of a helicopter. Airborne TIR was used to map spatial temperature patterns in the Methow River. TIR images were recorded during a three-day flight from August 24 to August 26, 2009 over the

Methow, Twisp, and Chewuch Rivers. A four mile reach of the Methow River near Winthrop is used to simulate the two-dimensional temperature dynamics downstream of the Chewuch River Spring Creek confluences.

Simulated 2D water temperature is compared to measured surface temperature to test the ability of the model in predicting lateral thermal mixing. Surface water temperature (measured) may be different than depth-averaged temperature (computed) due to stratification. This difference may cause some variance in how well the 2D model results can represent the TIR data, particularly in areas where the mixing rate of the river is slow or highly variable. The Methow is, however, generally well-mixed due to a steep slope and fairly shallow depths. For this reason, the surface water temperature is used for the model upstream boundary condition.

Two river gage stations are located in the study reach: USGS 12448500 (Methow at Winthrop downstream of the confluence of the Methow and Chewuch) and USGS 12448000 (Chewuch at Winthrop upstream of the confluence). On August 26, 2009, the flow rate of Methow at Winthrop was 275 cfs and that of Chewuch at Winthrop was 89.1 cfs (Table 4). The combined flow in the Methow River and Spring Creek above the Chewuch is obtained from the difference between the two gages. Then, the incoming discharge for Spring Creek and the Methow River was solved by assuming the incoming temperature and discharge product for each tributary equals the temperature and discharge product in the downstream river at the gage. The flow rates at the Methow River above the Chewuch is set as 146.0 cfs and the combined flows from Spring Creek is set as 40.8 cfs., to reach a mixed temperature downstream of the Spring Creek 15.8 ^{o}C from the surveyed data. The calculation assumed that there is no heat sources and sinks within this short reach.

Table 4 Incoming flow rates and temperatures.

	Flow Rate (cfs)	Temperature (^{o}C)
Chewuch	89.1	17.3
Methow	146.0	15.4
Spring Creek	40.8	13.6

Figures 1 through 3 display measured water surface temperature and simulated water temperature results. Figure 1 shows measured water surface temperature in the vicinity of the Chewuch and Spring Creek confluences. The field data indicates the presence of temperature mixing zones downstream of the tributary confluences; the comparatively small inflow from Spring Creek produces a low temperature zone that is highly persistent in the streamwise direction, suggesting non-point source seepage along the bank. Figure 2 shows the SRH-2D simulated temperature using point-based model contributions from the Chewuch and Spring Creek. The simulation results qualitatively reproduce the zone of lateral temperature stratification downstream of the Chewuch River, however vastly under predict the extent to which the cold temperature zone persists along the bank downstream of Spring Creek.

Figure 3 shows the SRH-2D numerical temperature simulation with a non-point source of water seeping into the stream from Spring Creek. From the calibration process, it was determined that a combination of 20.7 cfs modeled as point source from Spring Creek and 20 cfs modeled as non-point source seeps produces qualitative agreement with the measurements (Figure 1), predicting mixing zones from both tributaries fairly well.

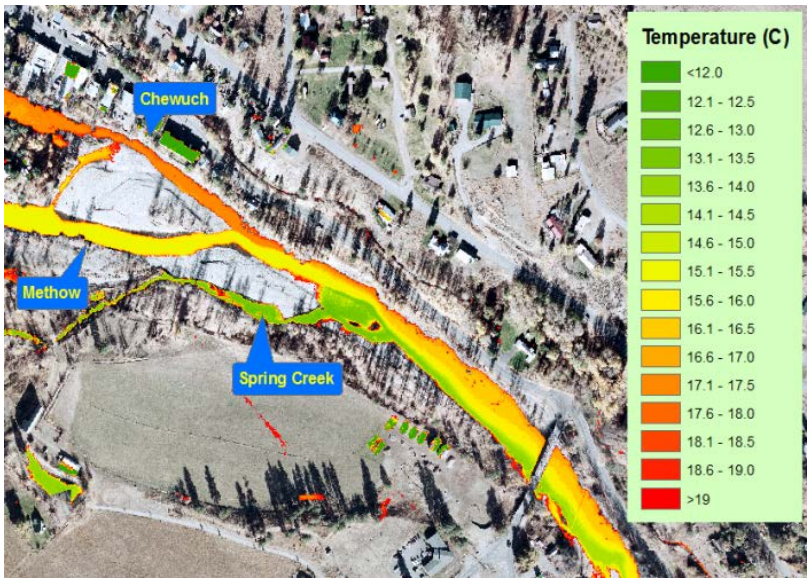

Figure 1 TIR imagery taken on August 26 2009 in the vicinity of the Chewuch River and Spring Creek. The color scale is mapped to measured water surface temperature. Warmer water from Chewuch River enters on the river left and colder water from the Spring Creek enters on the river right. Flow direction is from left to right.

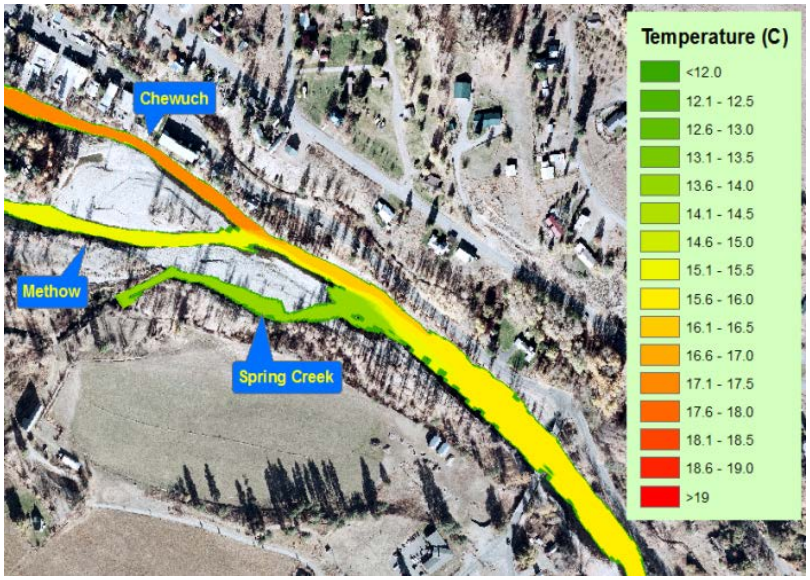

Figure 2 SRH-2D numerical simulation of water temperature at the confluences with the Chewuch River and the Spring Creek, with tributaries modeled as point sources. Color scale is mapped to predicted depth-averaged temperature. Flow direction is from left to right.

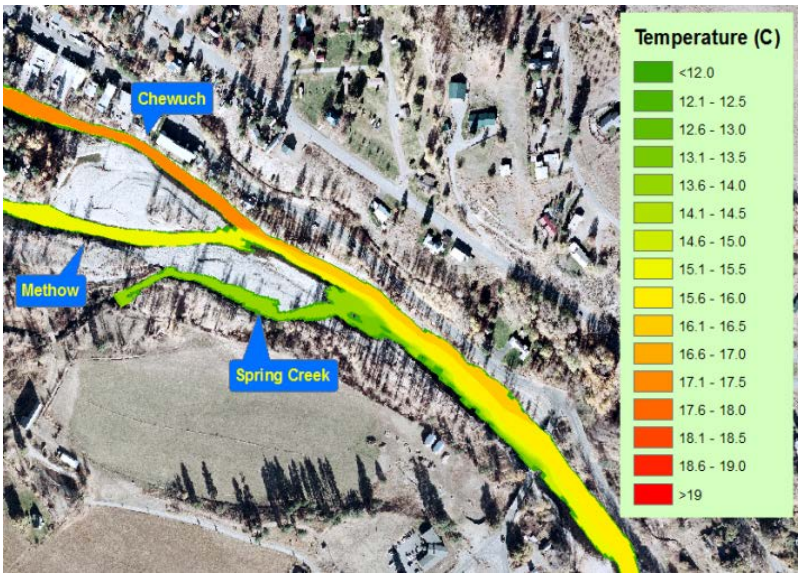

Figure 3 SRH-2D numerical simulation of water temperature at the confluences with the Chewuch River and the Spring Creek, with the Spring Creek contribution modeled as a combination of point-source and non-point source seeps from the right bank. Color scale is mapped to predicted depth-averaged temperature.

A sensitivity analysis was performed on the turbulent Prandtl number σ_t in Eq. (1). The turbulent Prandtl number is the ratio of momentum eddy diffusivity ν_t to thermal eddy diffusivity, and is typically on the order of one in natural turbulent flows. The results show that decreasing (increasing) the turbulent Prandtl number decreases (enlarges) the persistence of temperature gradients downstream of the tributary confluences.

Test Case with Log Data: In the second test case, SRH-2D is used to simulate unsteady flow and temperature over four months from June 1, 2012 to September 30, 2012. Several temperature loggers in the study reach provided continuous point temperature data that can be used to test model predictions of longitudinal changes in temperature. Three loggers provided continuous temperature measurements for upstream model boundary conditions at flow locations labeled Chewuch Mouth, Methow above Chewuch, and Spring Creek (Figure 4, Figure 5, and Table 5).

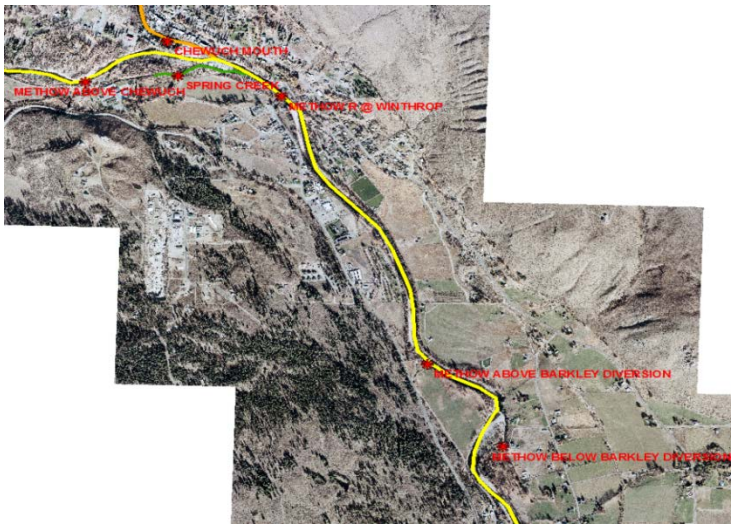

Figure 4 Temperature loggers located in the study reach.

Additional temperature logger data is needed to test model predictions along the channel. The logger location labeled Methow at Winthrop provided temperature downstream of the Chewuch and Spring Creek confluence at the US 20 bridge crossing in Winthrop. However, this location is in the temperature mixing zone; data was instead used from the logger located further downstream, labeled Methow above Barkley Diversion. Another logger, Methow below Barkley Diversion, located in the side channel which does not have a surface flow connection with the mainstem Methow River at the time of simulation and could not be used to test the model.

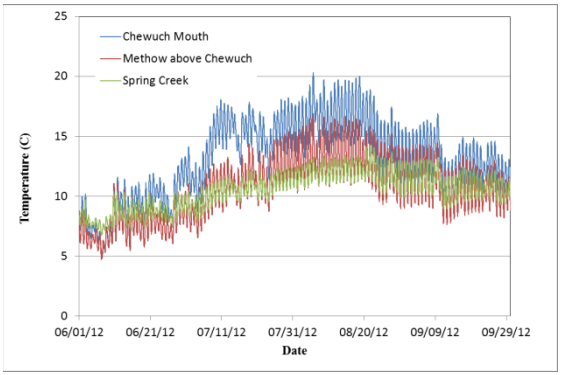

Figure 5 Methow, Chewuch, and Spring Creek inflow water temperatures used as upstream input boundary conditions for the model.

Table 5 Logger data available in the study reach.

Logger Location Label	Date Period
Chewuch Mouth	6/1/2005 to 9/18/2008, and 7/9/2010 to 10/11/2012
Methow Above Chewuch	6/30/2005 to 10/15/2009, and 7/16/2010 to 10/16/2012
Spring Creek	7/2/2005 to 10/15/2009, and 7/16/2010 to 10/16/2012
Methow at Winthrop	6/27/2005 to 10/13/2009
Methow above Barkley Diversion	11/26/2009 to 10/16/2012
Methow below Barkley Diversion	11/26/2009 to 10/16/2012

Two gage stations are located in the study reach (Figure 6): USGS 12448500 (Methow above Chewuch) and USGS 12448000 (Chewuch Mouth). There is no gage to measure flow in Spring Creek. The majority of the contribution from Spring Creek is due to ground seepage and the fish hatchery; further, there is no assumed correlation between the flow rates in the Methow and Spring Creek. For this reason, the same flow distribution used in the first test case was used in the second test case: 20.7 cfs from Spring Creek and 20 cfs from ground seepage on the right bank. Future field survey is recommended to measure the flow rate in the Spring Creek. The flow rate at the Methow above Chewuch is obtained by subtracting the flows at Chewuch and Spring Creek from the downstream gage at Methow at Winthrop.

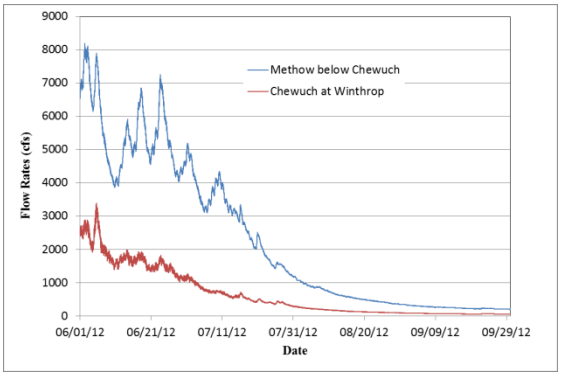

Figure 6 Methow and Chewuch River flow hydrographs used as upstream input boundary conditions.

The longitudinal temperature in the river is affected by the heat gain and loss at the water surface and channel bed. The dominant forms of heat gain are solar (short wave) radiation and atmospheric (long wave) radiation. The dominant forms of heat loss include back radiation from the stream, evaporative heat loss from the stream, and evaporative and conductive heat loss at the water surface. The heat flux to the channel bed is usually positive at day time and negative at night time. Solar radiation was not directly measured at the study reach, but was estimated from Eqs (6) to (21) given the cloud covering, elevation, and site latitude and longitude position.

Compared with logger data at the Methow above Barkley Diversion location, the model predicted the temperature fairly well Figure 7. The root mean square error is about 0.37^{o}C. No temperature difference was observed in the channel transverse direction (well-mixed) at the Methow above Barkley Diversion location. The wind effect coefficients a_1 and b_1 as defined in Eq. (24) were set as 1.0×10^{-9} and 1.0×10^{-9}, respectively. The coefficients were set to their low ends in order to maintain a slightly increased temperature in the downstream direction. To better understand the effects of all source terms, a longer reach is recommended. In a small reach, the meteorological effects are small and the temperature is more driven by the upstream boundary conditions.

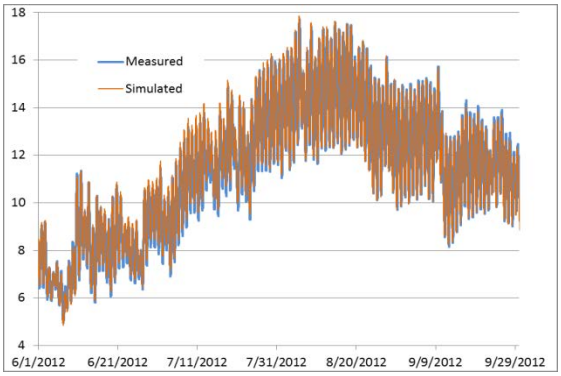

Figure 7 Measured and simulated water temperatures at the logger location labeled Methow above Barkley Diversion.

CONCLUSIONS

SRH-2D simulates the river temperature where water is well mixed in the vertical direction. First, the SRH-2D temperature module was tested using two sets of validation data from the Methow River near Winthrop, WA. Case one calculated a steady-state solution of the lateral temperature mixing zones downstream of the Chewuch (warmer water) and Spring Creek (colder water) confluences without any heat exchange with the air and channel bed. Case two calculated transient solutions of the temperature distribution driven by measured input hydrographs.
The model showed good accuracy in simulating the lateral temperature mixing zones downstream of tributary confluences when the model is well calibrated by adjusting the turbulent Prandtl number. In the Methow case, results show that the turbulent Prandtl number of one best reproduce the lateral temperature mixing. It was also shown that non-point source boundary conditions may be required to model spatially distributed contributions such as seepage of cold water from a spring.

The model was generally successful in reproducing the measured temporal variation in temperature measured at the Methow above Barkley Diversion location. In this four mile reach, the water temperature is mostly driven by incoming flow discharge and temperature, and not sensitive to weather/climate. For the Methow River, it is hypothesized from measured data that weather impacts to water temperature occur on the scale of multiple reaches, perhaps on the order of tens of river miles.

ACKNOWLEDGEMENTS

The authors would like to acknowledge the Research and Development Office, Science and Technology Program of the Bureau of Reclamation for providing funding to this research. The authors would like to thank Raymond “Jason” Caldwell, former employee of Bureau of Reclamation, who performed the research on modeling of daily and sub-daily stream temperatures which was used as input data in this study. The authors thank co-workers Yong

Lai, Blair Greimann, Dan Dombroski, and Subhrendu Gangopadhyay for discussions and insight. Dan Dombroski's peer review is appreciated.

REFERENCES

Hauser, G.E. and Schohl, G.A. (2003). "River Modeling System v4 – Vol. 2 Technical Reference," Report No. WR28-1-590-164, Tennessee Valley Authority, Norris, Tennessee.

Huber, W.C. and Harleman, D.R.F. (1968). "Laboratory and Analytical Studies of the Thermal Stratification in Reservoirs," Hydrodynamics Laboratory Technical Report No. 112, Department of Civil Engineering, Massachusetts Institute of Technology, Cambridge, Massachusetts, 277 pp.

Lai, Y., and Mooney, D. (2009). "On a Two-Dimensional Temperature Model: Development and Verification," World Environmental and Water Resources Congress, 1-14.

Marciano, J.J. and Harbeck, G.E. (1954). "Mass-transfer studies in Water-loss investigations—Lake Hefner studies". Technical Report: U.S. Geol. Survey Prof. Paper 269

Martin, J.L. and McCutcheon, S.C. (1999). "Hydrodynamics and Transport for Water Quality Modeling," CRC Press.

Rodi, W. (1993). "Turbulence models and their application in hydraulics," 3rd Ed., IAHR Monograph, Balkema, Rotterdam, The Netherlands.

Tung, C.P., Lee, T.Y., and Yang, Y.C. (2006). "Modeling climate-change impacts on stream temperature of Formosan landlocked salmon habitat," Hydrological Processes, Vol.20, 1629-1649.